Bulk Nuclear Polarization Enhanced at Room Temperature by Optical Pumping

Ran Fischer,[1] Christian O. Bretschneider,[2] Paz London,[1] Dmitry Budker,[3,4] David Gershoni,[1] and Lucio Frydman[2,*]

[1]*Department of Physics, Technion, Israel Institute of Technology, Haifa 32000, Israel*
[2]*Department of Chemical Physics, Weizmann Institute of Science, Rehovot 76100, Israel*
[3]*Department of Physics, University of California, Berkeley, California 94720-7300, USA*
[4]*Nuclear Science Division, Lawrence Berkeley National Laboratory, California 94720, USA*

Bulk ^{13}C polarization can be strongly enhanced in diamond at room temperature based on the optical pumping of nitrogen-vacancy color centers. This effect was confirmed by irradiating single crystals at a ~50 mT field promoting anticrossings between electronic excited-state levels, followed by shuttling of the sample into an NMR setup and by subsequent ^{13}C detection. A nuclear polarization of ~0.5%—equivalent to the ^{13}C polarization achievable by thermal polarization at room temperature at fields of ~2000 T—was measured, and its bulk nature determined based on line shape and relaxation measurements. Positive and negative enhanced polarizations were obtained, with a generally complex but predictable dependence on the magnetic field during optical pumping. Owing to its simplicity, this ^{13}C room temperature polarizing strategy provides a promising new addition to existing nuclear hyperpolarization techniques.

Introduction.—Nuclear magnetic resonance (NMR) is commonly used to extract molecular-level information in a wide variety of physical, chemical, and biological scenarios. One of NMR's most distinctive characteristics is the low energies it involves. This makes the method remarkably noninvasive but leads to intrinsically low signal-to-noise ratios (SNR), factoring in both small thermal spin polarizations and relatively low frequencies. Over the last decades several strategies have been proposed to bypass these limitations, particularly by generating large, non-thermal spin-polarized states. Most prominent among these techniques is dynamic nuclear polarization (DNP) [1–6], where radicals are irradiated in a high-field cryogenic environment, driving their unpaired electron spins away from equilibrium and thereby leading to highly polarized nuclei on co-mixed, nearby target molecules. This and other forms of hyperpolarization can increase NMR signals by several orders of magnitude, significantly expanding the scope of NMR applications in chemistry and biomedicine [7]. In the past, free radicals arising in imperfect diamond crystals have also been the target of cryogenic DNP NMR investigations [8,9]. Those studies have been recently extended to exploit the electronic spin states of negatively charged nitrogen-vacancy (NV) centers in diamond. These color centers have been proposed for a variety of applications including spintronics [10–14] and ultrasensitive magnetometry [15–18]. A particularly appealing aspect of NV centers is their efficient electronic polarization by optical pumping at room temperature; several studies have demonstrated that the ensuing electronic polarization can be transferred via hyperfine interactions to nearby nuclei and indirectly detected via the NV defects [19–23]. In this study we extend such experiments by

direct observations of the nuclear ^{13}C spins by means of NMR. To execute this polarization transfer, the NV centers are optically pumped by laser irradiation, and the electronic spin polarization was transferred to ^{13}C spins by aligning the diamond crystal in a magnetic field of ~50 mT. This leads to an excited-state level anticrossing (ESLAC), capable of polarizing ^{13}C spins exhibiting hyperfine couplings to the NV centers [19,24–27]. To characterize the enhanced nuclear polarization, an experimental setup was built which rapidly transferred the optically pumped NV-doped diamonds to a 4.7 T field. Once at high fields, the ^{13}C spins are excited using a resonant radio frequency (rf) pulse, and their nuclear polarization is detected by conventional NMR induction. The intensity of the NMR signal detected after optical pumping exceeded by 2–3 orders of magnitude the signal observed in the same setup after the sample was subject to full thermal relaxation in a 4.7 T field. It was found that the nuclear spins hyperpolarized by these optical means had the same NMR properties as bulk ^{13}C spins [28]. These included their relaxation, linewidth, and chemical-shift characteristics, which were found identical to those observed in thermally polarized high-field NMR experiments on the same sample. This "bulklike" behavior is further substantiated by experimental data suggesting that the majority of the observed hyperpolarized ^{13}C signal originates from nuclear spins located beyond 1 nm of the electronic paramagnetic defects. The nuclear polarization also revealed a complex dependence on the magnetic field strength during the optical pumping. This dependence, including NMR signal sign alternations, could be explained by the anisotropic nature of the electron-nuclear hyperfine interaction [29].

^{13}C *polarization enhancement method.*—The negatively charged NV color center in diamond is composed of a substitutional nitrogen atom associated with an adjacent lattice vacancy. This center is characterized by electronic spin triplets in both the ground ($^3A_2$) and the excited (^3E) state. At room temperature these $S = 1$ states exhibit zero-field splittings between the $m_S = 0$ and the $m_S = \pm 1$ spin sublevels of 2.87 and 1.42 GHz, respectively [Fig. 1(a)]. Optical transitions are primarily spin conserving [30,31]. However, the presence of a nonradiative, spin-selective relaxation mechanism involving an intersystem crossing with singlet levels leads upon optical pumping, to nearly fully polarized $m_s = 0$ electronic states even at room temperature. This electronic polarization can be transferred to nearby ^{13}C's in the diamond lattice by suitably tuning the external field [Fig. 1(b)]; transfers to nuclei possessing hyperfine couplings $\gtrsim 0.2\,\text{MHz}$ have thus been demonstrated [25]. To illustrate the nature of this transfer, we neglect for simplicity the ^{14}N-related spin interactions, and consider a single NV-^{13}C spin Hamiltonian

$$\hat{H} = D_{\text{ES}}\hat{S}_z^2 + (\gamma_{\text{NV}}\hat{S} + \gamma_{^{13}\text{C}}\hat{I}) \cdot \vec{B} + \hat{S} \cdot A_{\text{IS}} \cdot \hat{I}. \quad (1)$$

Here $\hat{I}$ and $\hat{S}$ are the nuclear and electron spin operators, D_{ES} is the excited-state zero-field splitting, $\gamma_{\text{NV}} = 2.8 \times 10^4$ MHz/T and $\gamma_{^{13}\text{C}} = 10$ MHz/T are the corresponding gyromagnetic ratios, and A_{IS} is the hyperfine tensor. Assuming an axial magnetic field $\vec{B} = B_z\hat{z}$, aligned with the NV axis, leaves the electronic spin an eigenstate of $\hat{S}_z$. In general, the zero-field and electronic Zeeman splitting dominating Eq. (1), suppresses electronic $\leftrightarrow$ nuclear spin exchanges. Still, as illustrated in Fig. 1(a), energy levels can be tuned with B_z: at a field of $\sim$50 mT the contributions of the first two terms in the electronic Hamiltonian

balance out for the electronic $\{|0\rangle, |-1\rangle\}$ subspace. This leads to an electronic anticrossing due to the presence of the hyperfine interaction with ^{13}C nuclei, resulting in a transfer between the optically pumped electronic and the nuclear spin populations $\{|\uparrow\rangle, |\downarrow\rangle\}$. Indeed, when $||D_{\text{ES}} - \gamma_{\text{NV}}B_z| \pm \gamma_{^{13}\text{C}}B_z| \approx |A_{\text{IS}}|$, the electronic spin is no longer an eigenstate of $\hat{H}$. The system can still be described in a joint manifold of the nuclear and electronic spins, but the eigenstates of $\hat{H}$ under these conditions are mixtures of the $|0,\uparrow\rangle$, $|0,\downarrow\rangle$, $|-1,\uparrow\rangle$ and $|-1,\downarrow\rangle$ states. If A_{IS} is a so-called isotropic hyperfine interaction possessing solely $\hat{S}_+\hat{I}_-$, $\hat{S}_-\hat{I}_+$ "zero-quantum" terms, only the $|-1,\uparrow\rangle$ and $|0,\downarrow\rangle$ states are mixed near the ESLAC, leading to an enrichment of the nuclear $|\uparrow\rangle$ state upon optical pumping [Fig. 1(b)]. By contrast, ^{13}C's exhibit both isotropic and anisotropic hyperfine characters [32], resulting in an additional mixing of states involving single- and double-quantum operators $\hat{S}_z\hat{I}_\pm$, $\hat{S}_\pm\hat{I}_z$, $\hat{S}_+\hat{I}_+$ and $\hat{S}_-\hat{I}_-$. Under optical pumping, these zero- and double-quantum terms can drive the nuclei into either polarized or antipolarized states [Fig. 1(b)]; the actual orientation depends on the magnitude of $\vec{B}$ and on the characteristics of A_{IS}. This is illustrated by toy-model simulations in Fig. 1(c), showing that multiple sign alterations in the nuclear spin polarization versus B_z can be expected, close to the anticrossing condition. This calculation is based on solving a master Liouville–von Neumann equation based on the Hamiltonian of Eq. (1). This in turn approximates the polarization buildup of the ^{13}C nuclear spins via a direct transfer process; its efficiency is determined by the magnitude of the hyperfine interaction, the lifetime ($\sim$10 ns) of the electronic excited state, and the pumping rate of the NV centers. The direct polarization process
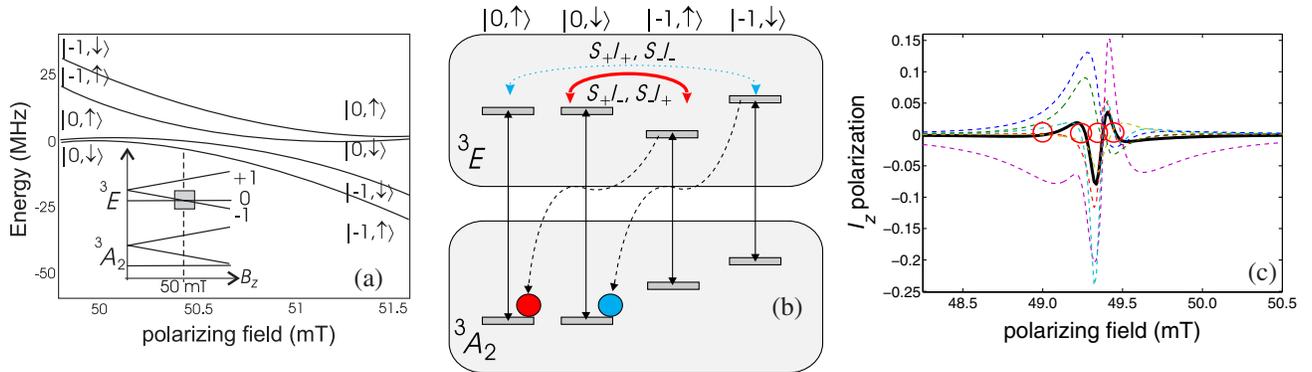

FIG. 1 (color online).   (a) Schematic energy diagram of the electronic ground ($^3A_2$) and excited (^3E) triplet states of an NV center at room temperature versus an axial magnetic field B_z. Numbers denote the electronic spin state, while arrows refer to nuclear spin-(1/2) ^{13}C. The magnified sketch shows the region of the ESLAC at approximately 50 mT. (b) Simplified schematic description of the polarization transfer processes between the electronic and nuclear substates under optical pumping in the presence of the hyperfine interaction. Vertical black solid (dashed) arrows represent optical (spin-selective) relaxation transitions, and horizontal red (cyan) arrows illustrate the mixing of the $|-1,\uparrow\rangle$ and $|0,\uparrow\rangle$ ($|-1,\downarrow\rangle$ and $|0,\downarrow\rangle$) energy levels, resulting in a positive (negative) nuclear polarization. (c) Nuclear polarizations of ^{13}C spins versus an axial magnetic field as determined by density matrix toy-model simulations. The bold line describes the mean polarization resulting from averaging over six individual orientations of the hyperfine tensor (dashed lines) [35]. Further details can be found in the Supplemental Material [28]. Notice the multiple zero crossings (red circles) of the nuclear polarization due to an effective averaging over subensembles with different hyperfine tensors.

facilitated by strong hyperfine interactions (> 0.2 MHz), was studied in [25]. In actuality, also weaker hyperfine interactions could enable a low-magnitude polarization transfer throughout the entire diamond sample—which although slow, would become significant once supported by long nuclear T_1 relaxation times. In addition, nuclear spin-diffusion events driven by $(\hat{I}_{1+}\hat{I}_{2-} + \hat{I}_{1-}\hat{I}_{2+})$-like terms originating from the nuclear dipole-dipole interaction, would also assist in transferring the nuclear polarization from strongly coupled ^{13}C's towards the bulk ^{13}C spin reservoir.

To investigate the existence and extent of these polarization transfer mechanisms, which could enable the pumping of significant bulk nuclear polarization by optical means, we assembled the setup illustrated in Fig. 2(a). The experiment began with alignment of an NV center-endowed diamond single crystal, in a $B_z \sim 50$ mT field fulfilling the ESLAC conditions [28]. Following laser irradiation, the sample was mechanically shuttled within subsecond time scales from the polarizing field to a detection field of 4.7 T. This motion positioned the diamond crystal within a ^{13}C-tuned Helmholtz-coil circuit; the experiment concluded with the application of an NMR spin-echo sequence to probe the level of ^{13}C magnetization.

Results and discussion.—NMR measurements on the samples, D02 and D01, revealed that an average bulk nuclear polarization of $\sim$0.50% and $\sim$0.12% was achieved by optical pumping of the NV centers. For D02 the ratio between the optically pumped signal and the signal observed in a thermally polarized ensemble at room temperature and 4.7 T, the so-called enhancement factor, was determined to be 486 ± 51 [28]. Taking into account the different polarizing and observation field strengths, the overall enhancement at 50 mT is $>10\,000$ times stronger than the B_z-derived prediction of the thermal Boltzmann polarization. This hyperpolarized ^{13}C signal showed identical characteristics as signals arising from thermally polarized high-field spin ensembles: within experimental errors, their chemical shift, spin-lattice relaxation times, and linewidths, are all identical [Figs. 3(a)–3(c)]. The ^{13}C polarization saturation, Fig. 3(d), suggests that the relatively short nuclear relaxation time at 50 mT ultimately limits the amount of electron polarization that can be transferred.

It follows that the hyperpolarized NMR signal observed is representative of (and therefore probably originates from) the ^{13}C bulk nuclei, rather than from a subset of nuclei in the immediate vicinity of the NV centers. By contrast, if the ^{13}C signal were to arise from the immediate surroundings of paramagnetic defects [e.g., $(A_{IS}/2\pi) \geq 10$ kHz] shorter relaxation times as well as hyperfine shifts would be expected driven by the electronic defects [28,33,34]. The origin of the enhanced nuclear polarization was further investigated by manipulating the nuclear spins with resonant, low-field rf pulses. In particular, a 180° pulse of a duration of $t_{180} \sim 90$ μs was applied at the nominal Larmor frequency of the ^{13}C spins at the 50 mT polarizing field. Such pulses are resonant solely with the nuclear spin population within its frequency bandwidth ($t_{180}^{-1} \sim 10$ kHz) and therefore will not affect ^{13}C spins exhibiting strong frequency shifts (e.g., by paramagnetic
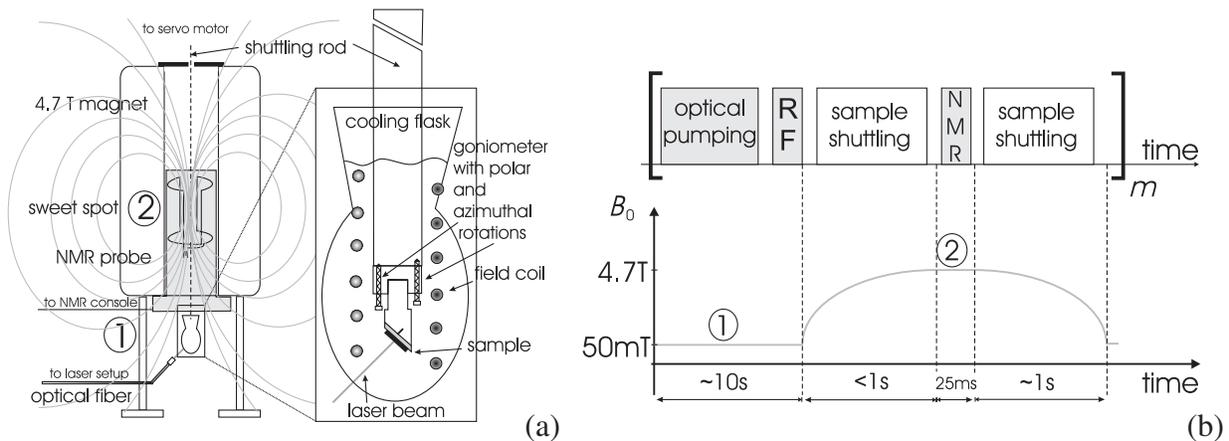

FIG. 2. (a)–(b) Schematic description of the experimental apparatus and sequence used in this Letter. Experiments begin with laser pumping of the electronic spins in a $\sim$50 mT axial field facilitating polarization transfer to the nuclear spins. (Nuclear spins could also be manipulated at this low field by applying resonant rf pulses at a frequency of $\sim$545 kHz). The sample is then shuttled from the polarizing field ① to the "sweet spot" of a high-field magnet ②, where ^{13}C spins are subject to a pulsed NMR detection. The sample returns to the polarizing field for a repeated pumping and further signal averaging. The samples used (D01, D02) are natural abundance ^{13}C single crystals exhibiting an estimated concentration of NV centers of 3 and 10 ppm, respectively, [28]. A 532 nm laser, delivering up to 10 W power was connected to the optical setup via an optical fiber irradiating an area slightly larger than the diamond sample. The polarizing field was fine tuned via an ancillary coil; during optical pumping, the sample was immersed in a water-filled flask to avoid excessive heating, and the concomitant distortion of the single-crystal alignment setup. The sample holder was connected by a shuttling rod to a servo motor enabling its transfer (in <1 s) into and out of high-field NMR setup. The ^{13}C polarization was monitored in this setup using an NMR probe enabling free shuttling through a Helmholtz coil configuration tuned to 50.55 MHz.
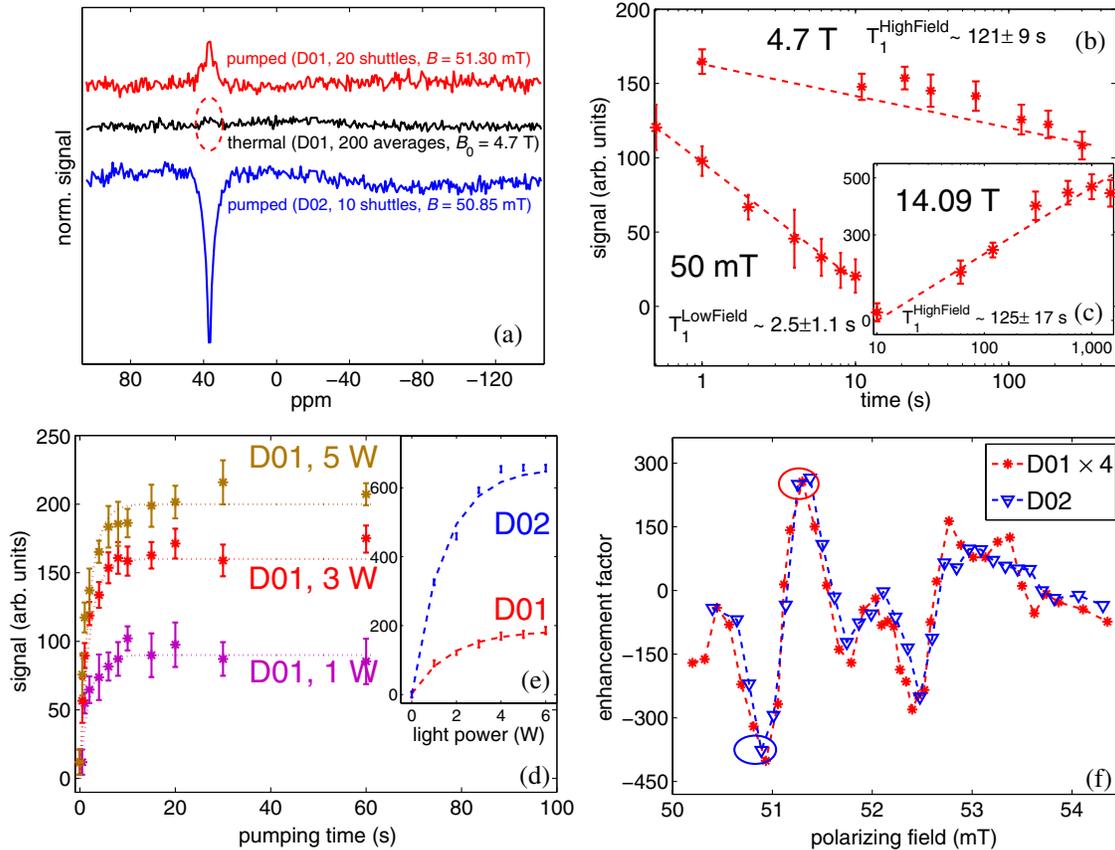
FIG. 3 (color online). Measured experimental data of the diamond samples D01 (red lines, asterisks) and D02 (blue lines, triangles). The dashed lines are guides for the eye. (a) ^{13}C signal (red and blue line) obtained after 10 s of optical pumping and ^{13}C signal acquired at 4.7 T for the diamond D01 (black line). The positive and negative polarizations correspond to different polarizing fields and the dashed oval marks the position of the NMR signal, corresponding to the thermal Boltzmann polarization of the sample. (b) Spin-lattice relaxation characteristics of the optically pumped signal of the sample D01. The longitudinal relaxation of the ^{13}C polarization was measured at the two turning points of the shuttling process marked as ① and ② in Figs. 2(a) and 2(b): the polarizing field, and the observation field (see [28] for similar data from sample D02). (c) Saturation-recovery of bulk ^{13}C obtained under conventional thermal polarizing conditions on a high-field solid-state spectrometer ($B_0 = 14.09$ T). (d,e) Build-up characteristics of the optically pumped ^{13}C polarization versus irradiation time for various laser-beam powers, and versus light power after 10 sec of pumping. (f) The enhancement of the ^{13}C SNR as a function of the polarizing field. The spectra shown in panel (a) correspond to the encircled points: red circle $B_z = 51.30$ mT, blue circle $B_z = 50.85$ mT). Notice that the enhancement of D01 is shown magnified $4 \times$.

sources). The application of such a pulse during the course of low-field optical pumping (in which the majority of the NV centers are found in $m_S = 0$ state, devoid of hyperfine interaction) should result in an inversion of the entire macroscopic ^{13}C polarization. By contrast, if the rf pulse is applied after the laser illumination has ended and the electronic population has returned to a thermal Boltzmann distribution, only ^{13}C spins with hyperfine couplings weaker than the 10 kHz Rabi frequency would experience a full inversion. Hence, this experiment distinguishes between nuclear populations with hyperfine interactions stronger and weaker than ~10 kHz. Measuring the high-field NMR signals in the presence and absence of these low-field pulses reveals a full nuclear population flip (See Supplemental Material 3 in [28]). This confirms that a majority of the hyperpolarized signal originates from ^{13}C spins with hyperfine interactions <10 kHz, corresponding to a minimum distance ≥ 1 nm from diamond NV defects.

An additional feature worth noting is the control in the relative sign of the ^{13}C magnetization provided by the polarization field. This prediction is implied by the "toy" simulations in Fig. 1(c), and demonstrated experimentally in Fig. 3(f). The observed dependence of the ^{13}C polarization on the magnetic field resembles the predictions based on Eq. (1), but exhibits several additional zero crossings. These sign alternations in the nuclear polarization were identical for both diamond crystals D01 and D02 [Fig. 3(f)]. This implies that the observed bulk nuclear polarization reflects a general (albeit complex) behavior that the multiple ^{13}C subspecies coupled by an anisotropic hyperfine interaction with an NV center, undergo at each resonance instance [25]. Indeed, the possible positions of ^{13}C nuclei in the diamond crystal with respect to an NV center, result in an array of individual hyperfine interactions. Different magnetic field conditions will result for each of these cases, leading to a distinct pattern for the ensuing electronic-nuclear polarization transfer.

Conclusions.—This study shows that in a single-crystal room temperature diamond, a significant ^{13}C nuclear polarization can be established within seconds, by optical pumping of NV centers at a suitable magnetic field. From this observation, many additional interesting paths emerge both regarding basic features of NV-driven nuclear enhancement, and in the synergies between this method of spin polarization and magnetic-resonance experiments. Foremost among these are alternative routes to enhance even further the bulk ^{13}C polarization; either by manipulating the concentration of NV centers, by ^{13}C enrichment, or by choosing different irradiation, field or temperature conditions during the pumping. Strategies can also be envisioned for transferring the ^{13}C polarization from the diamond to other molecules, or for using the diamond as a reporter of NMR properties while remaining at low magnetic fields. Interesting opportunities for studies of basic characteristics of spin-spin driven transfers within the diamond as well as to chemical and biological molecules are opened. These and other alternatives to enable a better understanding and a wider use of this polarizing technique, are being investigated.

*lucio.frydman@weizmann.ac.il

[1] J. H. Ardenkjær-Larsen, B. Fridlund, A. Gram, G. Hansson, M. H. Lerche, R. Servin, M. Thaning, and K. Golman, Proc. Natl. Acad. Sci. U.S.A. **100**, 10 158 (2003).

[2] J. Wolber et al., Nucl. Instrum. Methods Phys. Res., Sect. A **526**, 173 (2004).

[3] K. Golman, R. in't Zandt, and M. Thaning, Proc. Natl. Acad. Sci. U.S.A. **103**, 11 270 (2006).

[4] C. G. Joo, K. N. Hu, J. Bryant, and R. Griffin, J. Am. Chem. Soc. **128**, 9428 (2006).

[5] S. Bowen and C. Hilty, Angew. Chem., Int. Ed. **47**, 5235 (2008).

[6] J. Leggett, R. Hunter, J. Granwehr, R. Panek, A. J. Perez-Linde, A. J. Horsewill, J. McMaster, G. Smith, and W. Köckenberger, Phys. Chem. Chem. Phys. **12**, 5883 (2010).

[7] J. Kurhanewicz et al., Neoplasia **13**, 81 (2011).

[8] E. C. Reynhardt and G. L. High, J. Chem. Phys. **109**, 4090 (1998); **109**, 4100 (1998).

[9] L. B. Casabianca, A. I. Shames, A. M. Panich, O. Shenderova, and L. Frydman, J. Phys. Chem. C **115**, 19 041 (2011).

[10] A. Gruber, A. Dräbenstedt, C. Tietz, L. Fleury, J. Wrachtrup, and C. von Borczyskowski, Science **276**, 2012 (1997).

[11] R. J. Epstein, F. M. Mendoza, Y. K. Kato, and D. D. Awschalom, Nat. Phys. **1**, 94 (2005).

[12] L. Childress, M. V. Gurudev Dutt, J. M. Taylor, A. S. Zibrov, F. Jelezko, J. Wrachtrup, P. R. Hemmer, and M. D. Lukin, Science **314**, 281 (2006).

[13] M. V. Gurudev Dutt, L. Childress, L. Jiang, E. Togan, J. Maze, F. Jelezko, A. S. Zibrov, P. R. Hemmer, and M. D. Lukin, Science **316**, 1312 (2007).

[14] R. Hanson, V. Dobrovitski, A. Feigun, O. Gywat, and D. Awschalom, Science **320**, 352 (2008).

[15] J. M. Taylor, P. Cappellaro, L. Childress, L. Jiang, D. Budker, P. R. Hemmer, A. Yacoby, R. Walsworth, and M. D. Lukin, Nat. Phys. **4**, 810 (2008).

[16] J. R. Maze et al., Nature (London) **455**, 644 (2008).

[17] G. Balasubramanian et al., Nature (London) **455**, 648 (2008).

[18] V. M. Acosta, E. Bauch, A. Jarmola, L. J. Zipp, M. P. Ledbetter, and D. Budker, Appl. Phys. Lett. **97**, 174104 (2010).

[19] V. Jacques, P. Neumann, J. Beck, M. Markham, D. Twitchen, J. Meijer, F. Kaiser, G. Balasubramanian, F. Jelezko, and J. Wrachtrup, Phys. Rev. Lett. **102**, 057403 (2009).

[20] P. Neumann, J. Beck, M. Steiner, F. Rempp, H. Fedder, P. R. Hemmer, J. Wrachtrup, and F. Jelezko, Science **329**, 542 (2010).

[21] J. P. King, P. J. Coles, and J. A. Reimer, Phys. Rev. B **81**, 073201 (2010).

[22] P. London, J. Scheuer, J.-M. Cai, I. Schwarz, A. Retzker, M. B. Plenio, T. Katagiri, T. Teraji, S. Koizumi, J. Isoya, R. Fischer, L. P. McGuinness, B. Naydenov, and F. Jelezko, arXiv:1304.4709.

[23] E. Togan, Y. Chu, A. Imamoglu, and M. D. Lukin, Nature (London) **478**, 497 (2011).

[24] B. Smeltzer, L. Childress, and A. Gali, New J. Phys. **13**, 025021 (2011).

[25] A. Dréau, J.-R. Maze, M. Lesik, J. F. Roch, and V. Jacques, Phys. Rev. B **85**, 134107 (2012).

[26] B. Smeltzer, J. McIntyre, and L. Childress, Phys. Rev. A **80**, 050302 (2009).

[27] R. Fischer, A. Jarmola, P. Kehayias, and D. Budker, Phys. Rev. B **87**, 125207 (2013).

[28] See Supplemental Material at http://link.aps.org/supplemental/10.1103/PhysRevLett.111.057601 for further information on the alignment process by means of optical detection, density matrix simulations, estimation of the enhancement factor, and the average number of spins polarized per NV center.

[29] H.-J. Wang, C. S. Shin, C. E. Avalos, S. J. Seltzer, D. Budker, A. Pines, and V. S. Bajaj, Nat. Commun. **4**, 1940 (2013).

[30] N. B. Manson, J. P. Harrison, and M. J. Sellars, Phys. Rev. B **74**, 104303 (2006).

[31] M. W. Doherty, N. B. Manson, P. Delaney, and L. C. L. Hollenberg, New J. Phys. **13**, 025019 (2011).

[32] S. Felton, A. M. Edmonds, M. E. Newton, P. M. Martineau, D. Fisher, D. J. Twitchen, and J. M. Baker, Phys. Rev. B **79**, 075203 (2009).

[33] E. C. Reynhardt and C. J. Terblanche, Chem. Phys. Lett. **269**, 464 (1997).

[34] A. Dréau, P. Spinicelli, J. R. Maze, J. F. Roch, and V. Jacques, Phys. Rev. Lett. **110**, 060502 (2013).

[35] L. Childress, Ph.D. thesis, Harvard University, 2006, p. 52.